

## Percolation at the surface of semi-infinite two-dimensional lattices

B. P. Watson

*Department of Physics, St. Lawrence University, Canton, New York 13617*

(Received 18 November 1985)

The method of Monte Carlo invariant imbedding is developed to calculate the probability that a site on the surface of a semi-infinite, two-dimensional lattice belongs to the bulk infinite cluster. For the square and triangular lattices, the surface percolation exponent is found to be  $\beta_1 = 0.398 \pm 0.005$ . This result is compared with those found indirectly using scaling relations on different surface exponents obtained by other methods.

### I. INTRODUCTION

When an infinite system is terminated by a surface to form a semi-infinite system, some features of its critical behavior are modified. A case in point is a lattice that has a fraction  $p$  of its sites randomly occupied, the rest being vacant. The fraction of sites that belong to the infinite cluster is called the percolation probability  $P(p)$ . It is commonly known<sup>1</sup> that  $P(p)$  is nonzero only if  $p$  is greater than a critical concentration  $p_c$  and that in a critical region above  $p_c$  the percolation probability has the power-law form

$$P(p) \propto (p - p_c)^\beta. \tag{1}$$

For a lattice with a free surface,  $P_1(p)$  is the probability that a site on the surface belongs to the infinite cluster; for ease of reference, such percolating sites are often called wet. By analogy with Eq. (1),

$$P_1(p) \propto (p - p_{c1})^{\beta_1}. \tag{2}$$

It is commonly assumed that  $p_{c1} = p_c$  and since the results confirm it, no further distinction will be made between the critical concentrations.

That  $P_1(p) \leq P(p)$  can be understood by visualizing the serpentine nature of the infinite cluster near the percolation threshold: Figure 1 illustrates how some wet sites will become dry when an infinite system is cut to form a surface. While the inequality could be satisfied by supposing different proportionality constants for Eqs. (1) and (2), it is the case that  $\beta_1 > \beta$ , and so the percolation transition at the surface is softer than that of the bulk.

Critical behavior at surfaces and methods for calculating the host of associated critical exponents have been reviewed by Binder.<sup>2</sup> The surface exponents are related to each other and to the bulk exponents by a collection of scaling relations such that if only one of the surface exponents is known the others may be determined.<sup>3</sup> Series expansions<sup>4</sup> and renormalization-group methods<sup>3</sup> have been used to obtain the susceptibility (mean-size) exponents  $\gamma_1$  and  $\gamma_{11}$ , and from these  $\beta_1$  may be found. Mean-field theories<sup>5,6</sup> yield  $\beta_1 = \frac{3}{2}$ . Carton<sup>7</sup> has derived a first-order  $\epsilon$  expansion for  $\beta_1$  which, however, can hardly be very accurate in two dimensions. At present, values for  $\beta_1$  are known less accurately than for the bulk counter-

parts and the best values are obtained only indirectly via the scaling relations.

I present here a new method for directly calculating precise values for the surface percolation probability exponent  $\beta_1$ . I apply the method to the semi-infinite square and triangular lattices and compare the results with those obtained indirectly by other methods.

### II. INVARIANT IMBEDDING

The method of invariant imbedding has great power for calculating surface properties of semi-infinite systems. Problems in fields as diverse as electron backscattering<sup>8</sup> and transmission-line impedance<sup>9</sup> have found solutions by this approach. For a review, see Ref. 10. For the present problem the basic idea is shown in Fig. 2. A set of func-

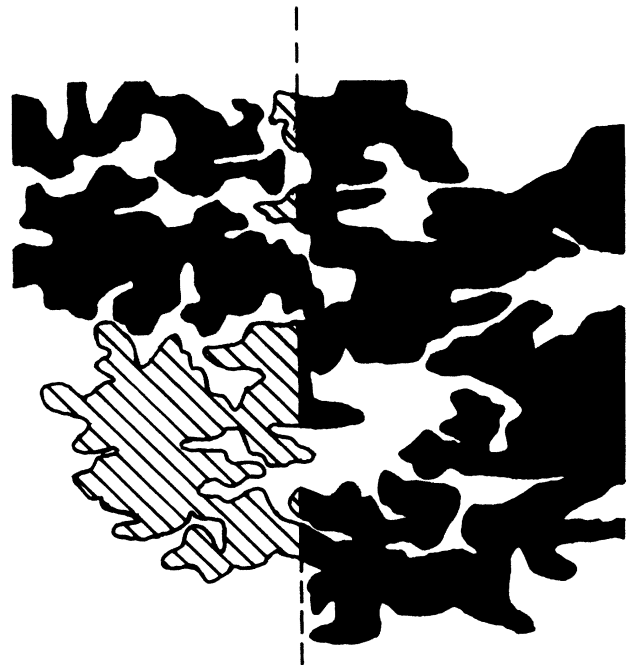


FIG. 1. A stylized piece of the infinite cluster. The hatched area shows the portion that becomes detached when the cluster is cut along the dashed line.

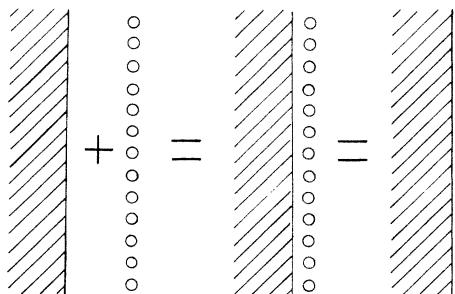


FIG. 2. Schematic representation of invariant imbedding at a surface.

tions  $\{P_i\}$  is defined which completely characterizes the surface of a semi-infinite system. Each  $P_i$  depends in an unknown way (which we wish to discover) upon a set of independent intensive variables  $\{x\}$ . A new surface is created by adding to the old surface a thin layer of material having the same values for  $\{x\}$ . Each function  $P'_j$  of the new surface is then assumed to be related to the old set  $\{P_i\}$  and to  $\{x\}$ :

$$P'_j = f_j(\{P_i\}, \{x\}), \tag{3}$$

but the addition of the layer leaves the system still semi-infinite, so we require that each of the surface functions be unchanged, and

$$P'_j = P_j \tag{4}$$

for each  $j$ . Equations (3) and (4) are the central ideas of invariant imbedding in the present context.

The relations expressed in Eq. (3) depend on the details of the structure of the layer and how the layer interacts with the old surface. Constructing these relations is usually a formidable task, and it is not often obvious at the outset what to choose as the set  $\{P_i\}$ . Consider the semi-infinite, two-dimensional square lattice, each site of which is occupied with probability  $p$ . The goal is to determine  $P_1(p)$ , the probability that a surface site is wet. In this case there is only one independent intensive variable, the occupation probability  $p$ . An attempt to write down Eq. (3) for  $P'_1$  will necessarily involve a whole collection of surface correlation functions each of which is related to the others by invariant-type equations. So that the method may be illustrated, these complexities are swept aside by ignoring correlations among wet sites: In what follows it is assumed that the wet sites are randomly distributed on the surface.

Figure 3 shows the possible configurations of wet sites for a small portion of the surface three sites wide. Connections to sites that border this portion are ignored. Sites on the old surface are wet with probability  $P_1$ . To the right of the dashed line a new column of sites (with occupation probability  $p$ ) is appended to make a new surface. By enumerating the configurations and writing down their probability of occurrence, one obtains the probability that the center site of the new surface is wet:

$$P'_1 = P_1 p + P_1(1 - P_1)(2p^2 - p^3 P_1). \tag{5}$$

The first term in Eq. (5) is just the probability that the in-

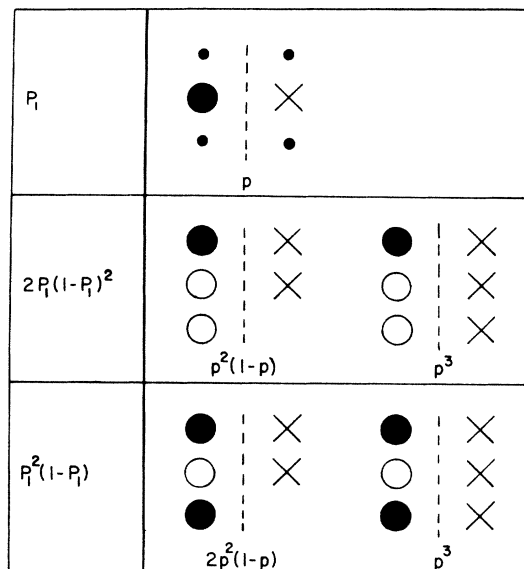


FIG. 3. Propagation of the wet cluster for a three-site portion of the surface. ●, wet site; ○, non-wet site; ×, occupied site on new surface; ●, site of irrelevant status. Expressions in left-hand column are probabilities for topologically distinct configurations of sites on the old surface. Expressions below each diagram give probabilities for site configuration on the new surface.

finite cluster is propagated directly forward as shown in the first row of Fig. 3. The second term results from adding all of the probabilities for the remaining configurations.

Upon setting  $P'_1 = P_1$ , Eq. (5) may be simplified to obtain a quadratic equation in  $P_1$  whose coefficients are po-

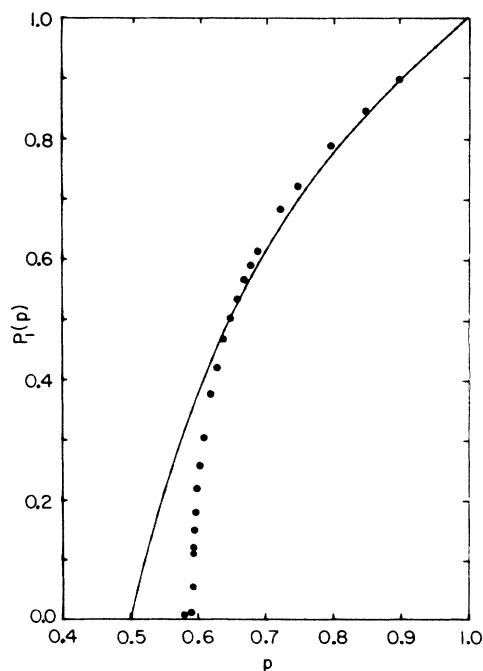


FIG. 4. Variation of surface percolation probability with site concentration for the square lattice. Solid line is the result of the analytical model of Eq. (6). Data points show typical Monte Carlo simulations of Sec. III.

ynomials in  $p$ . The solution is

$$P_1 = \frac{p(p+2) - (p^4 - 4p^3 + 4p)^{1/2}}{2p}, \quad (6)$$

which is plotted as the solid line in Fig. 4. Equation (6) has the correct behavior of  $P_1 \sim p$  in the limit  $p \rightarrow 1$  where correlations can be ignored, and it provides a reasonable approximation to the true surface percolation probability outside of the critical region. But it fails, not unexpectedly, to yield the correct critical concentration or power-law behavior.

By using surface portions larger than three sites it is possible to write down higher-order approximations but they quickly become unwieldy. Furthermore, such approximations are bound to fail in the critical region unless they are based on a very wide surface and account for correlations. A more promising approach is to carry out the invariant imbedding procedure by computer simulation.

### III. MONTE CARLO INVARIANT IMBEDDING

The goal is to model Eqs. (3) and (4) numerically. The basic strategy is very simple. If a surface has the correct fraction of wet sites properly correlated then a new layer added to the surface will attain the same fraction of wet sites. This information is, of course, unavailable at the outset. However, by starting with an arbitrary concentration and distribution of wet sites we hope that, after adding many new layers, the distribution will converge to the correct one. Whether this does occur may be judged by the numerical results presented here.

Consider an initial column of  $N$  surface sites which is randomly populated with a fraction  $P(p,0)$  of wet sites. A new column, occupied with sites with probability  $p$ , is adjoined to the initial column. The wet cluster and other finite clusters are propagated forward into the new column wetting a fraction  $P(p,1)$  of the sites on the new surface. The process is repeated through  $K$  iterations, giving a sequence  $P(p,1), P(p,2), \dots, P(p,K)$ . This procedure was implemented with a cluster-propagation algorithm based on the Hoshen-Kopelman technique and similar to that given by Stauffer.<sup>11,12</sup> There were several differences, however. Rather than just determining if the new column was connected to the first column, the number of sites so connected was counted. Cluster numbers were recycled. Rapaport<sup>13</sup> has shown that periodic boundary conditions produce more accurate cluster-size distributions than free-boundary conditions. In this work, it was convenient to use almost-periodic boundary conditions in which the  $N$ th site of the  $K$ th column abuts the first site of the  $(K+1)$ th column. This introduces a screw dislocation of pitch  $1/N$  which can be ignored for the large column lengths used here.

For finite  $N$ , the value of  $P(p,K)$  does not converge to a fixed value but fluctuate about an average value which approximates  $P_1(p)$ . Most of the difficulties with the method concern knowing when the sequence has converged to the vicinity of this average value. In preliminary simulations, an initial column of  $N=1000$  was populated randomly with  $P(p,0)=p$ . For each value of  $p$ , en-

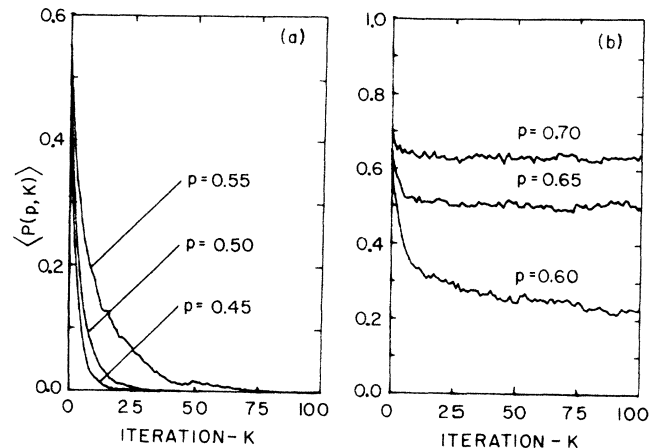


FIG. 5. Convergence of fraction of wet surface sites to an invariant value. (a)  $p < p_c$  and (b)  $p > p_c$ .

sembles of twelve runs were averaged. Typical ensemble averages  $\langle P(p,K) \rangle$  are plotted against iteration number in Fig. 5(a) for  $p < p_c$  and Fig. 5(b) for  $p > p_c$ . Below  $p_c$ , the original "infinite" cluster refuses to propagate. Above  $p_c$ , there is an initial steep, relatively smooth decrease followed by a more gradual, fluctuating decline and eventually by a fluctuation about an average value.

Starting with  $P(p,0)=p$  is a good approximation for high concentrations, but in the critical region this choice means starting from a very-high-concentration fluctuation in the infinite cluster. In addition, a diverging correlation length also slows convergence dramatically as  $p_c$  is approached. To speed convergence, a trial function  $f(p)=A(p-p_c)^\beta$  was fitted to preliminary data in the critical region. Then more extensive data were taken using the starting condition  $P(p,0)=f(p)$ . The effect is to start the system near its average value but without regard to correlations. That the proper correlations develop by themselves as the sequence progresses is probably a valid assumption provided that the sequence number  $K$  is carried at least past the mean cluster-size radius. Representative data for the square lattice are shown in Fig. 4.

A column length of  $N=10000$  was chosen for final simulations on the square and triangular lattices.<sup>14</sup> The surface percolation probability was approximated by the sequence average

$$\langle P_1(p) \rangle = \sum_{K=K_i}^{K_f} P(p,K) / (K_f - K_i + 1), \quad (7)$$

where  $K_i=1001$  and  $K_f=5000$ . The first 1000 sequence values were omitted to assure convergence to an approximately invariant distribution. Estimates for the variance in  $\langle P_1 \rangle$  were obtained by taking averages over subsets of the data.

### IV. RESULTS

Data for the square and triangular lattices are presented in Fig. 6, where for each lattice  $p_c^*$  was chosen which produced the least weighted  $\chi^2$  for an assumed linear rela-

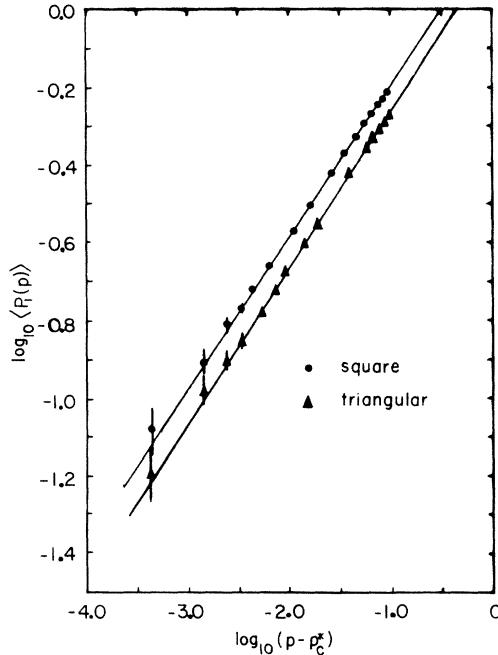


FIG. 6. Power-law behavior of  $\langle P_1(p) \rangle$  for the square and triangular lattices.  $p_c^*$  was chosen to achieve best linear fit.

tionship between  $\log_{10} \langle P_1 \rangle$  and  $\log_{10}(p - p_c^*)$  over a critical range of  $p - p_c^* \equiv \epsilon \lesssim 0.06$ . The data exhibit linear behavior over nearly two-and-a-half decades of  $\log_{10} \epsilon$ . Weighted least-squares analysis was used to find the best values for the constants in the fitting function  $P_1(p) = A_1(p - p_c^*)^{\beta_1}$ . These are listed in Table I with the most precise values for  $p_c$  obtained by other methods. The values for the exponent  $\beta_1$  are very nearly the same for the two lattices. However, the numbers obtained depend slightly on the range of data used in fitting and on the value of  $p_c^*$ . If these additional uncertainties are taken into account the data support the universality hypothesis that the two lattices have the same exponent.

For each lattice,  $p_c^*$  is greater than  $p_c$  by about 0.12%. This difference was found to be twice as large for another series of runs on the triangular lattice using a column length of only 1000, so the difference is probably due to the effect of finite sample size. In each instance  $\log_{10} \langle P_1 \rangle$  begins to lie slightly above the straight-line fit for  $\log_{10} \epsilon \lesssim -2.5$ . This signals the onset of a correlation

TABLE I. Least-squares values for the fitting function  $P_1(p) = A_1(p - p_c^*)^{\beta_1}$ .

	Square lattice	Triangular lattice
$\beta_1$	$0.392 \pm 0.005$	$0.403 \pm 0.004$
$A_1$	$1.57 \pm 0.02$	$1.38 \pm 0.02$
$p_c^*$	$0.5935 \pm 0.0002$	$0.5006 \pm 0.0002$
$p_c$	$0.59277 \pm 0.00005^a$	$\frac{1}{2}^b$

<sup>a</sup>Reference 15.

<sup>b</sup>Exact result.

TABLE II. Summary of results for the surface percolation probability exponent.

	$\beta_1$
This work	$0.398 \pm 0.005^a$
Series expansions (triangular lattice)	$0.382 \pm 0.005^b$ $0.43 \pm 0.02^c$
Renormalization group (square lattice)	$0.48^d$

<sup>a</sup>Average of values of Table I.

<sup>b</sup>Equation (9a);  $\gamma_{11} = 0.57 \pm 0.01$  (Ref. 4).

<sup>c</sup>Equation (9b);  $\gamma_1 = 2.10 \pm 0.02$  (Ref. 4).

<sup>d</sup>Equation (9c);  $\Delta_1 = \nu_b^p / \nu_b^b = 0.71 / 0.61$ ,  $\nu_b = 1 / \nu_b^b = 1 / 0.61$  (Ref. 3).

length approaching the value of  $K_i$  in Eq. (7) and indicates that convergence may not have been obtained. The toe evident at  $p < p_c$  in Fig. 4 is a more dramatic result of convergence failure. Other deviations from simple power-law behavior, barely discernible on Fig. 6, occur for  $\epsilon \gtrsim 0.07$ . These merely mark the end of the critical region for which Eq. (2) is valid.

These results for  $\beta_1$  are the first obtained directly for two-dimensional lattices. However,  $\beta_1$  can be calculated from the knowledge of one of the other surface exponents and the following scaling relations:<sup>3</sup>

$$\beta_1 = 2 - \alpha_s - \Delta_1,$$

$$\gamma_{11} = \alpha_s - 2 + 2\Delta_1,$$

(8)

$$\gamma_1 = \alpha_s - 2 + \Delta_b + \Delta_1,$$

$$2 - \alpha_s = (d - 1)\nu_1 = (d - 1)\nu_b,$$

where the subscript  $b$  denotes values of the bulk exponents.<sup>16</sup> For  $d = 2$  dimensions these equations can be manipulated to give

$$\beta_1 = \frac{1}{2}(\nu_b - \gamma_{11}),$$

(9a)

$$\beta_1 = \Delta_b - \gamma_1,$$

(9b)

and

$$\beta_1 = \nu_b - \Delta_1.$$

(9c)

The values  $\nu_b = \frac{4}{3}$  and  $\Delta_b = \frac{91}{36}$  are presumed to be known exactly.<sup>11,17,18</sup> The mean-size exponents  $\gamma_1$  and  $\gamma_{11}$  have been obtained from series expansions.<sup>4</sup> The exponent  $\Delta_1$  can be obtained from renormalization-group calculations.<sup>3</sup>

In Table II, I compare the values of  $\beta_1$  obtained by these other methods with the result of Monte Carlo invariant imbedding. None of the ranges for  $\beta_1$  overlap. However, the two series-expansion results do span the present value. The discrepancies are probably systematic: The renormalization-group calculation used a small cell size and the series expansions may have been too short.<sup>2</sup> The invariant imbedding value is subject to finite-size effects and a convergence uncertainty.

## V. CONCLUSION

The method of Monte Carlo invariant imbedding provides a new approach for calculating precise values of the surface percolation exponent. The results for the square and triangular lattices are very close and have an average of  $\beta_1 = 0.398 \pm 0.005$ , which is probably more accurate than values obtained indirectly by other methods. The invariant imbedding approach need not be limited to calculating percolation probabilities. Work is currently underway to calculate the mean-size exponents  $\gamma_1$  and  $\gamma_{11}$ . Eff-

ort will be directed toward extension to three and higher dimensions where the surface scaling relations are untested.

## ACKNOWLEDGMENTS

I thank T. F. Anderson for his able assistance with data analysis and Dr. H. Nakanishi for valuable discussions. This research was supported in part by a grant from Research Corporation.

<sup>1</sup>For recent reviews, see J. W. Essam, *Rep. Prog. Phys.* **43**, 833 (1980); D. Stauffer, *Phys. Rep.* **54**, 1 (1979).

<sup>2</sup>K. Binder, in *Phase Transitions and Critical Phenomena*, edited by C. Domb and J. L. Lebowitz (Academic, London, 1983), Vol. 8, p. 1.

<sup>3</sup>K. De'Bell, *J. Phys. C* **13**, 3809 (1980).

<sup>4</sup>K. De'Bell and J. W. Essam, *J. Phys. C* **13**, 4811 (1980).

<sup>5</sup>K. De'Bell and J. W. Essam, *J. Phys. A* **14**, 1993 (1981).

<sup>6</sup>A. Theumann, *Phys. Rev. B* **19**, 6295 (1979).

<sup>7</sup>J. P. Carton, *J. Phys. Lett.* **41**, 175 (1980).

<sup>8</sup>Roger F. Dashen, *Phys. Rev.* **134**, A1025 (1964).

<sup>9</sup>John J. Karakash, *Transmission Lines and Filter Networks* (MacMillan, New York, 1950), p. 161.

<sup>10</sup>R. Bellman, R. Kalaba, and G. Wing, *J. Math. Phys.* **1**, 280

(1960).

<sup>11</sup>D. Stauffer, in *Disordered Systems and Localization*, edited by C. Castellani, C. DiCastro, and L. Peliti (Springer-Verlag, Berlin, 1981), p. 9.

<sup>12</sup>J. Hoshen and R. Kopelman, *Phys. Rev. B* **14**, 3438 (1976).

<sup>13</sup>D. C. Rapaport, *J. Phys. A* **18**, L175 (1985).

<sup>14</sup>It is most convenient to propagate the triangular lattice in the [11] direction.

<sup>15</sup>T. Gebele, *J. Phys. A* **17**, L51 (1984).

<sup>16</sup>It is assumed that the surface correlation-length exponent  $\nu_1$  does not differ from the bulk value  $\nu_b$ .

<sup>17</sup>Robert B. Pearson, *Phys. Rev. B* **22**, 2579 (1980).

<sup>18</sup>B. Nienhuis, E. K. Riedel, and M. Schick, *J. Phys. A* **13**, L189 (1980).